Is it thermally inverted or not? The KELT-7b atmospheric conundrum revisited with CHEOPS, TESS, and additional data

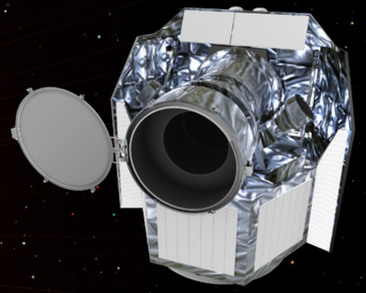

Z. Garai,
A. Krenn, P. E. Cubillos, G. Bruno, A. M. S. Smith, T. G. Wilson, A. Brandeker, M. N. Günther,
A. Heitzmann, L. Carone, V. Singh, M. Lendl, O. D. S. Demangeon, and the CHEOPS consortium



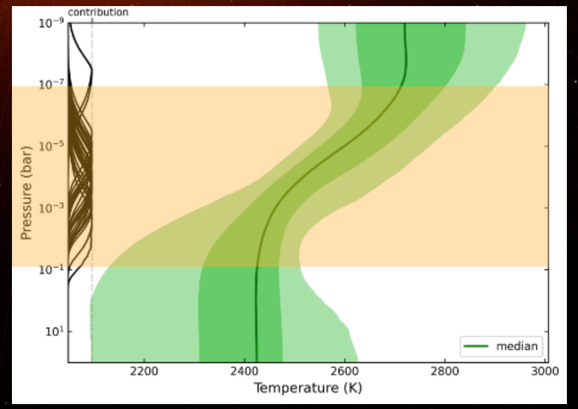

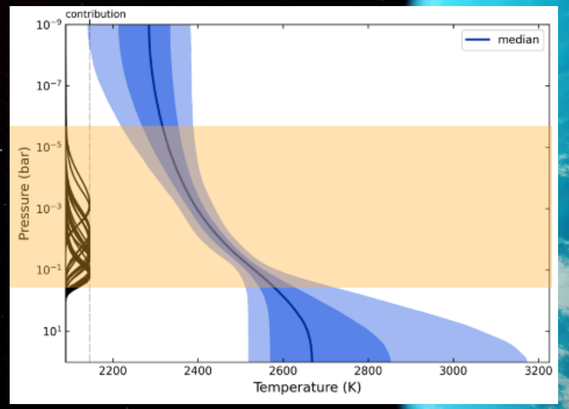

Institute seminar, Astronomical Institute, Slovak Academy of Sciences,
Tatranská Lomnica, December 17, 2025

A&A, 700, A5 (2025)
https://doi.org/10.1051/0004-6361/202452560
© The Authors 2025

Astronomy & Astrophysics

The KELT-7b atmospheric thermal-inversion conundrum revisited with CHEOPS, TESS, and additional data★

Z. Garai[1,2,3,★★], A. Krenn[4], P. E. Cubillos[4,5], G. Bruno[6], A. M. S. Smith[7], T. G. Wilson[8], A. Brandeker[9], M. N. Günther[10], A. Heitzmann[11], L. Carone[4], V. Singh[6], M. Lendl[11], O. D. S. Demangeon[12,13], Y. Alibert[14,15], R. Alonso[16,17], J. Asquier[10], T. Bárczy[18], D. Barrado[19], S. C. C. Barros[12,13], W. Baumjohann[4], W. Benz[15,14], N. Billot[11], L. Borsato[20], C. Broeg[15,14], A. Collier Cameron[21], A. C. M. Correia[22], Sz. Csizmadia[7], M. B. Davies[23], M. Deleuil[24], A. Deline[11], B.-O. Demory[14,15], A. Derekas[2,51], B. Edwards[25], J. A. Egger[15], D. Ehrenreich[11,26], A. Erikson[7], J. Farinato[20], A. Fortier[15,14], L. Fossati[4], M. Fridlund[27,28], D. Gandolfi[29], K. Gazeas[30], M. Gillon[31], M. Güdel[32], Ch. Helling[4,33], K. G. Isaak[10], F. Kerschbaum[32], L. L. Kiss[34,35], J. Korth[36], K. W. F. Lam[7], J. Laskar[37], A. Lecavelier des Etangs[38], D. Magrin[20], P. F. L. Maxted[39], B. Merín[40], C. Mordasini[15,14], V. Nascimbeni[20], G. Olofsson[9], R. Ottensamer[32], I. Pagano[6], E. Pallé[16,17], G. Peter[41], D. Piazza[42], G. Piotto[20,43], D. Pollacco[8], D. Queloz[44,45], R. Ragazzoni[20,43], N. Rando[10], H. Rauer[7,46], I. Ribas[47,48], N. C. Santos[12,13], G. Scandariato[6], D. Ségransan[11], A. E. Simon[15,14], S. G. Sousa[12], M. Stalport[49,31], S. Sulis[24], Gy. M. Szabó[2,1], S. Udry[11], S. Ulmer-Moll[11,15,49], V. Van Grootel[49], J. Venturini[11], E. Villaver[16,17], N. A. Walton[50], S. Wolf[42], D. Wolter[7], and T. Zingales[43,20]

(Affiliations can be found after the references)

Received 10 October 2024 / Accepted 21 May 2025

The KELT-7 planetary system

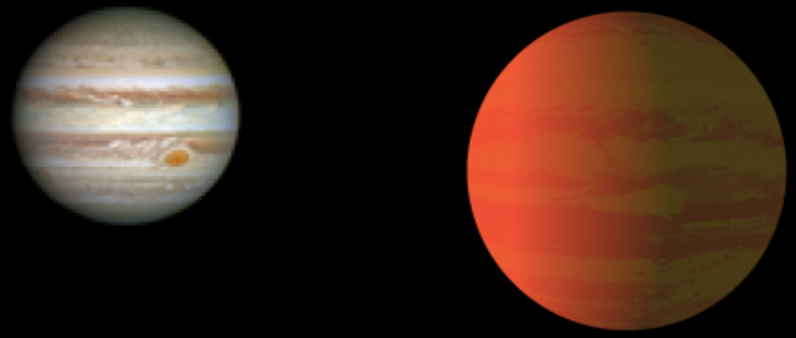

Image credit: NASA ESA A. Simon

Jupiter vs KELT-7 b

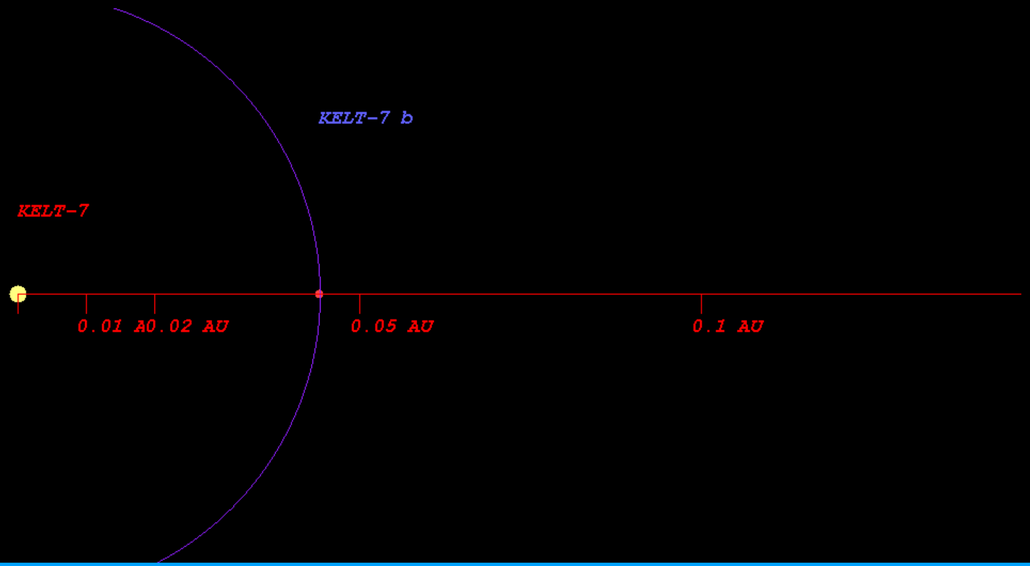

- KELT-7b is a transiting exoplanet (Bieryla et al. 2015):

orbital period: $P_{\rm orb} \sim 2.734\,{\rm d}$,

mass: $M_{\rm p} \sim 1.28\,{\rm M_{Jup}}$,

radius: $R_{\rm p} \sim 1.496\,{\rm R_{Jup}}$.

- It is an ultrahot Jupiter with $T_{\rm eq} = 2028 \pm 17\,{\rm K}$ (Tabernero et al. 2022), transiting a bright ($V = 8.54\,{\rm mag}$), rapidly rotating F2V-type star KELT-7.

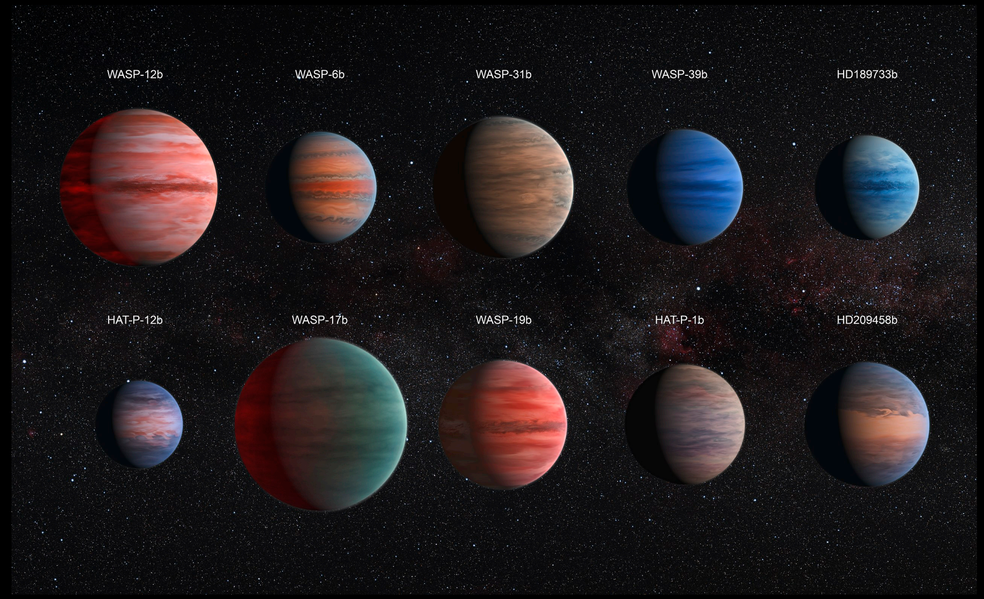

- **Hot Jupiters** (HJs) are giant gaseous planets, similar to Jupiter, but orbiting very close to their host stars. They have short orbital periods ($P_{\rm orb}$ = 1-5 d) and high equilibrium temperatures ($T_{\rm eq}$ = 1500-2500 K).

- **Ultrahot Jupiters** (UHJs) with hot ($T_{\rm eq} > 2000\,{\rm K}$) and extended atmospheres are ideal targets for atmospheric characterization.

- KELT-7b: bright host star (ideal for CHEOPS, TESS) + short orbit + high temperature.

Characterization methods of exoplanetary atmospheres

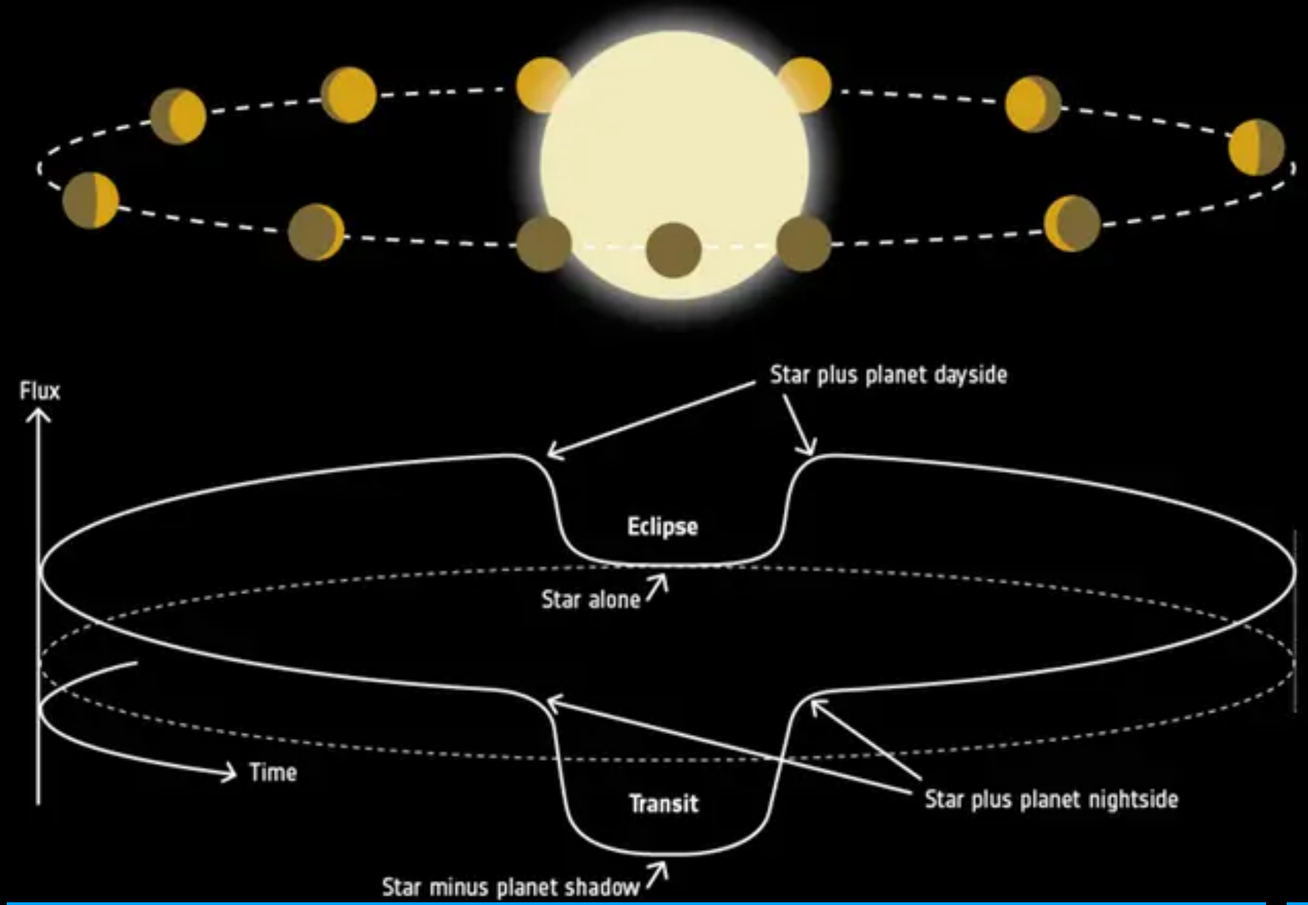

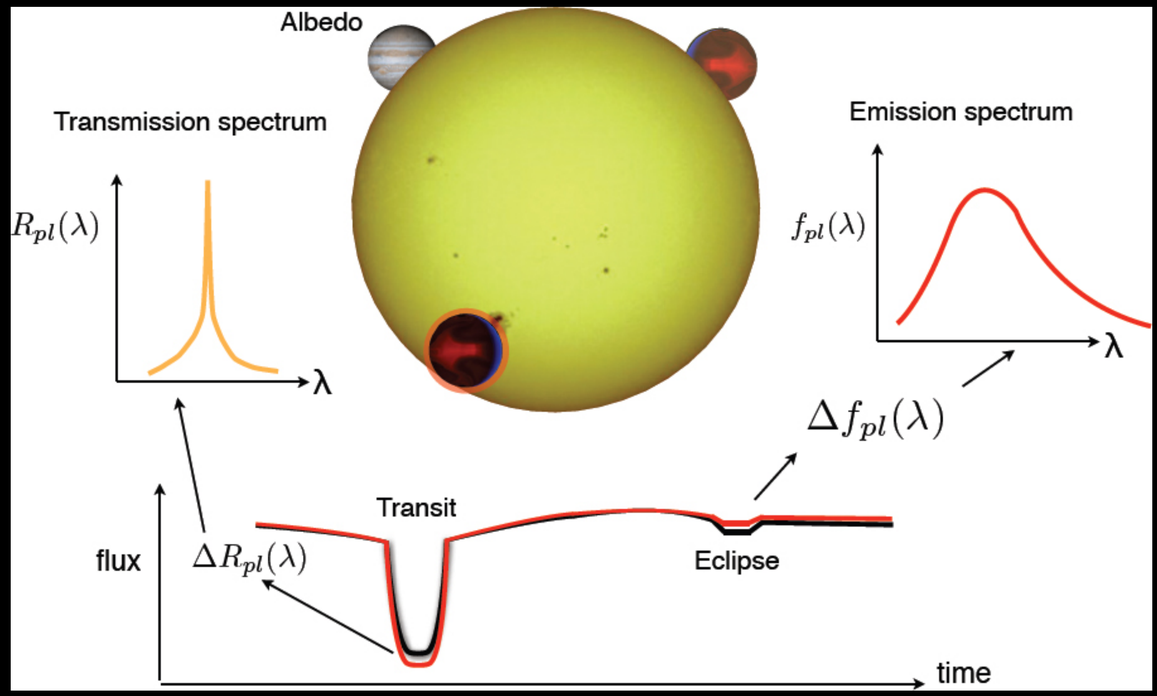

<u>Transmission spectroscopy:</u>
- measures the wavelength-dependent depth of the transit,
- is sensitive to the atmospheric composition at 0.1-1000 mbar, along the day-night terminator,
- is sensitive to clouds and high-altitude hazes;
- detections: several atomic and molecular species, such as Na, K, TiO, H_2O, CO, CO_2.

<u>Emission spectroscopy:</u>
- measures the wavelength-dependent depth of the secondary eclipse (occultation),
- brings information about the global properties of the planet's dayside atmosphere (dayside compisition),
- is sensitive to the vertical temperature-pressure (T-P) profile of the atmosphere.

- The occultation depth can be translated into a **<u>geometric albedo</u>** (A_g), which is the albedo of the planet at full phase (occultation), if only reflected light is measured, or if thermal emission contribution is accounted for.

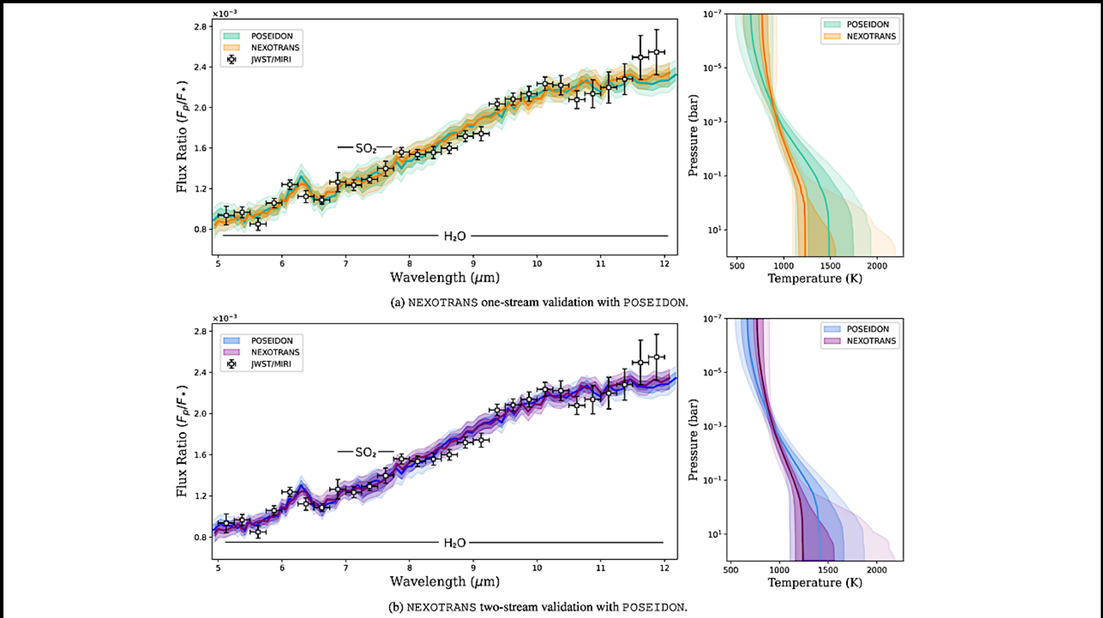

(a) NEXOTRANS one-stream validation with POSEIDON.

(b) NEXOTRANS two-stream validation with POSEIDON.

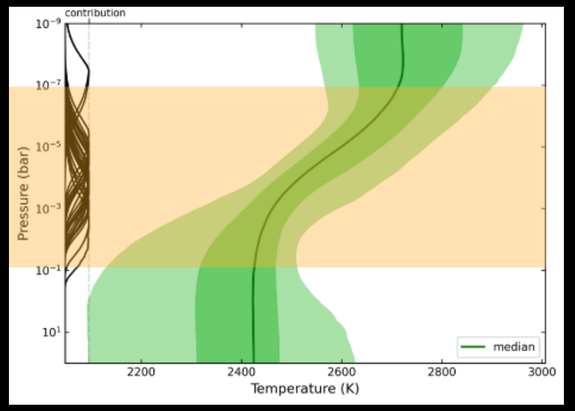

Inverted T-P profile

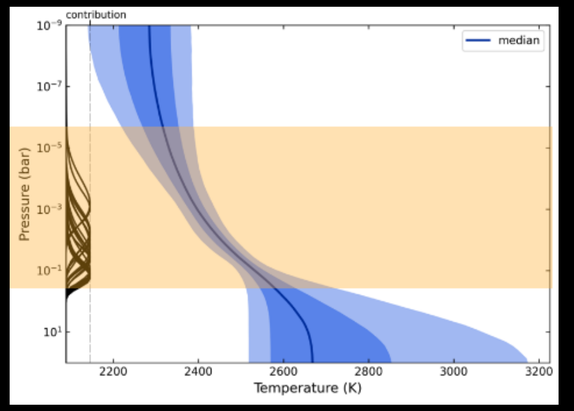

Normal T-P profile

- Emission spectroscopy is sensitive to the vertical T-P profile:
- **thermal inversions** can be detected:
elevated temperatures at low pressures.

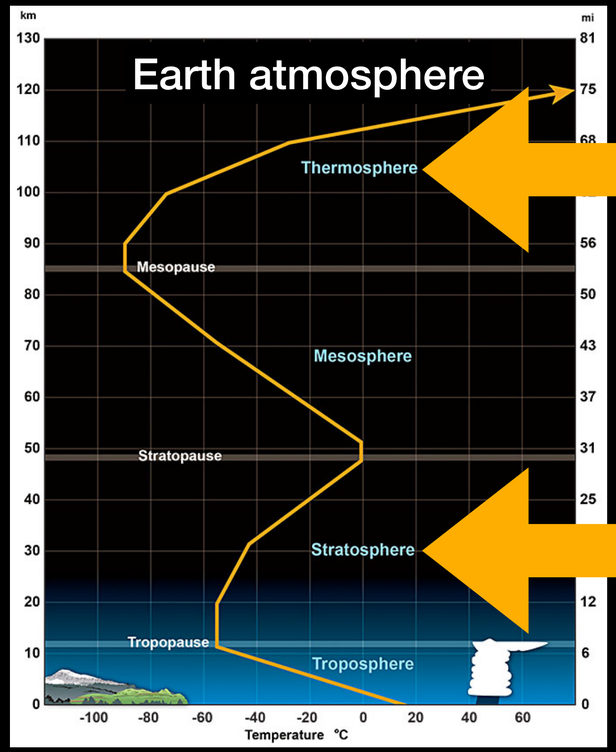

Absorption of
EUV/X-ray radiation
by atoms/molecules/ions

Absorption of
UV radiation by O_3

- Early theoretical works suggested that UHJs have inverted T-P profiles in the presence of optical absorbers, such as TiO and VO (Hubeny et al. 2003, Fortney et al. 2008),
- H^- was also considered (e.g., Lothringer et al. 2018),
- TiO might not play a role in the upper atmosphere (e.g., Spiegel et al. 2009),
- the diagnosis is a model-dependent process (Madhusudhan et al. 2014).

- Thermal inversions were usually found in UHJs: WASP-33b, WASP-121b, WASP-103b, KELT-9b, …
- But there are exceptions (e.g., WASP-12b).

- Exceptions at UHJs,
- uncertain absorbers,
- model-dependency

empahasize the importance of such detections.

KELT-7b is an UHJ, and an ideal target (relatively bright star):
1.) characterize the atmosphere of KELT-7b,
2.) derive the T-P profile,
3.) provide a precise measurement of the albedo of KELT-7b.

Aims

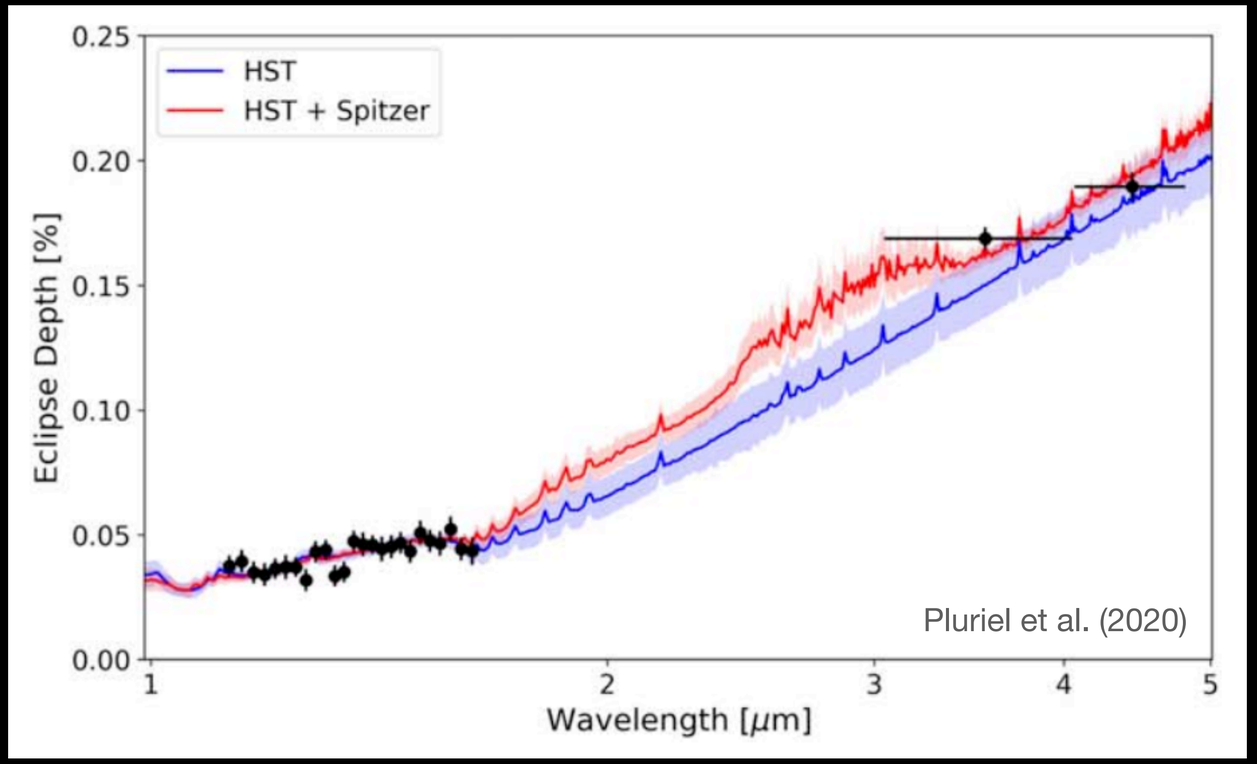

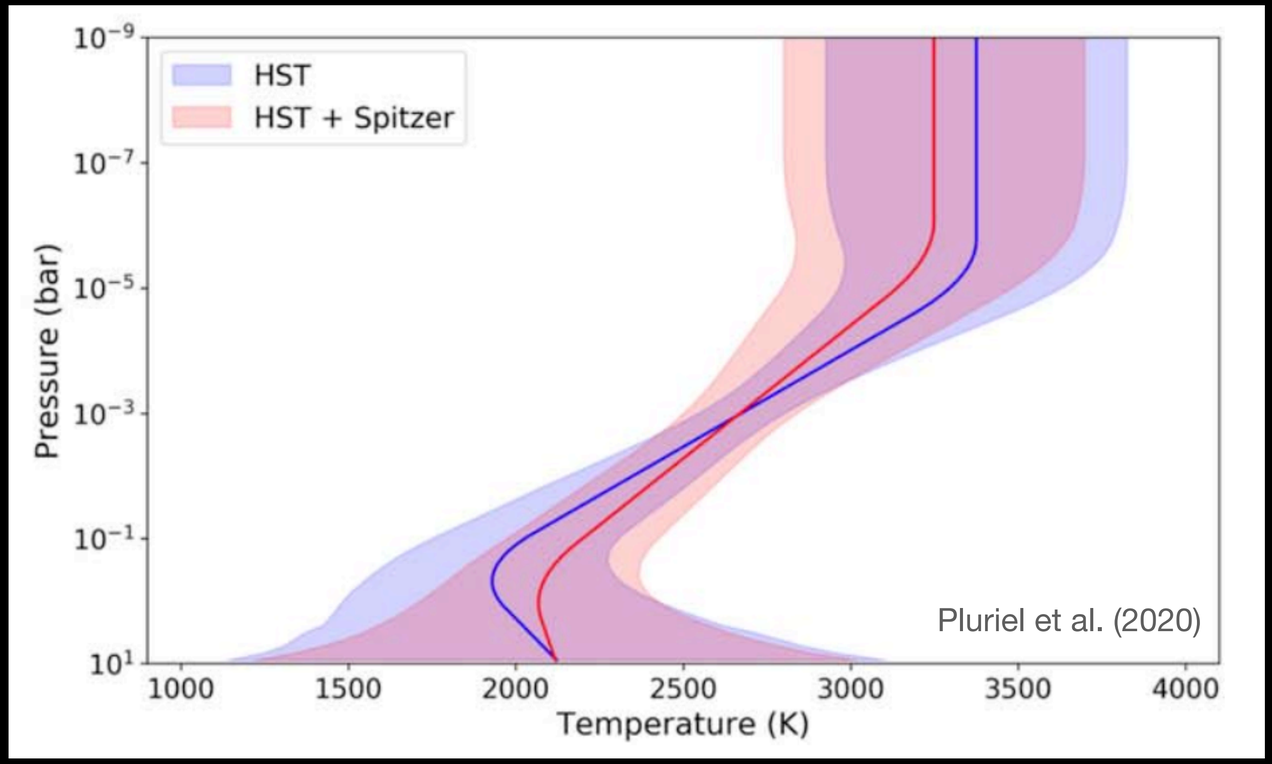

Recently, Pluriel et al. (2020) and Changeat et al. (2022) analyzed the atmosphere of KELT-7b:
- based on the HST and Spitzer occultations,
- detected an inverted T-P profile,
- found a non-detection of H_2O and a detection of H^- absorption.

4.) compare our results and the recently published results.

Observations

Optical observations:

1.) 12 occultation observations of KELT-7b with CHEOPS (λ = 330-1100 nm, blue sensitive),

2.) 2 transit observations of KELT-7b with CHEOPS (λ = 330-1100 nm, blue sensitive),

3.) TESS data (PDCSAP flux) from 7 sectors (λ = 600-1000 nm, red sensitive).

Infrared observations:

4.) Garhard et al. (2020): Spitzer InfraRed Array Camera (IRAC) transit/occultation observations ($\lambda \sim 3.6\,\mu$m and $\lambda \sim 4.5\,\mu$m),

5.) Pluriel et al. (2020): HST Wide Field Camera 3 (WFC3) transit/occultation observations ($\lambda \sim 1.12 - 1.63\,\mu$m).

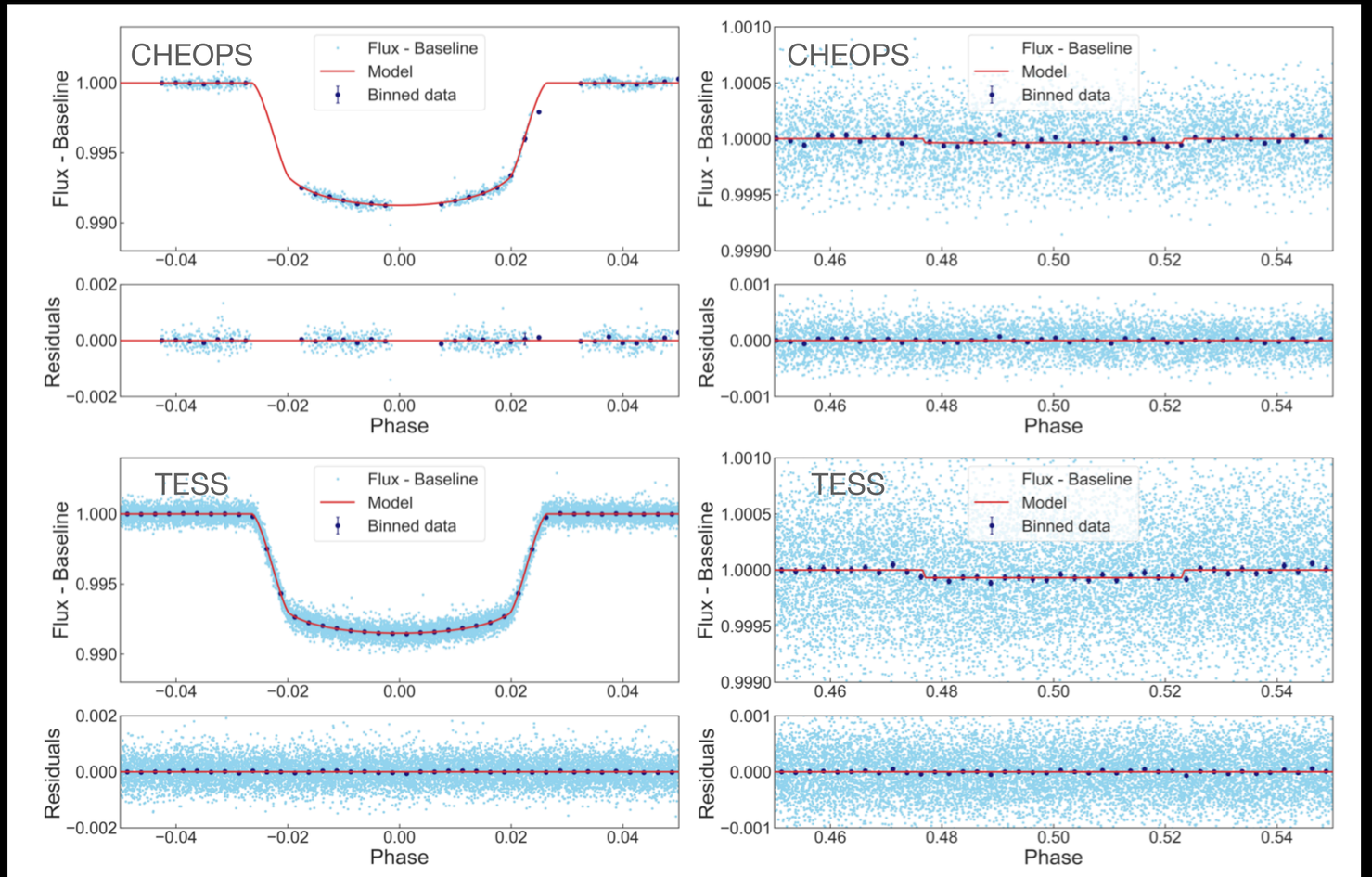

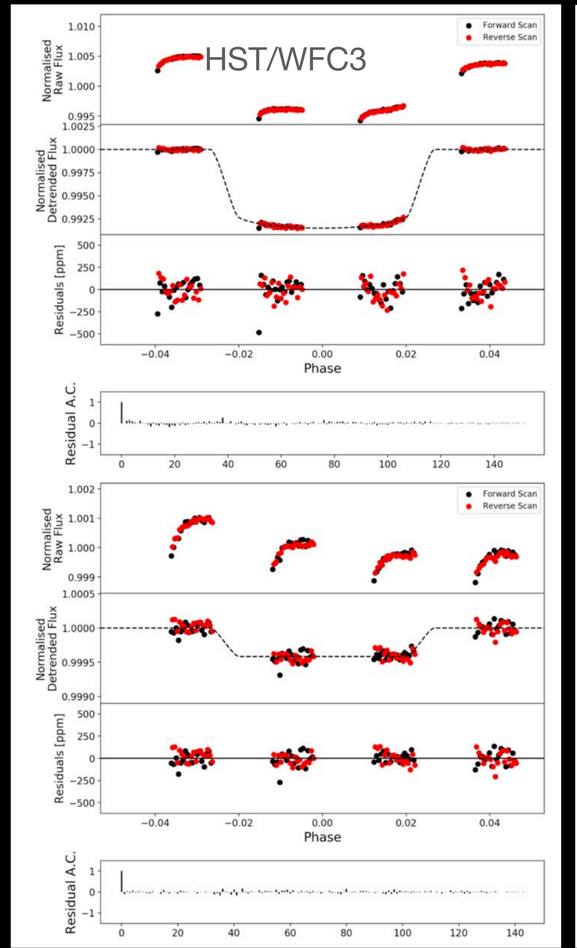

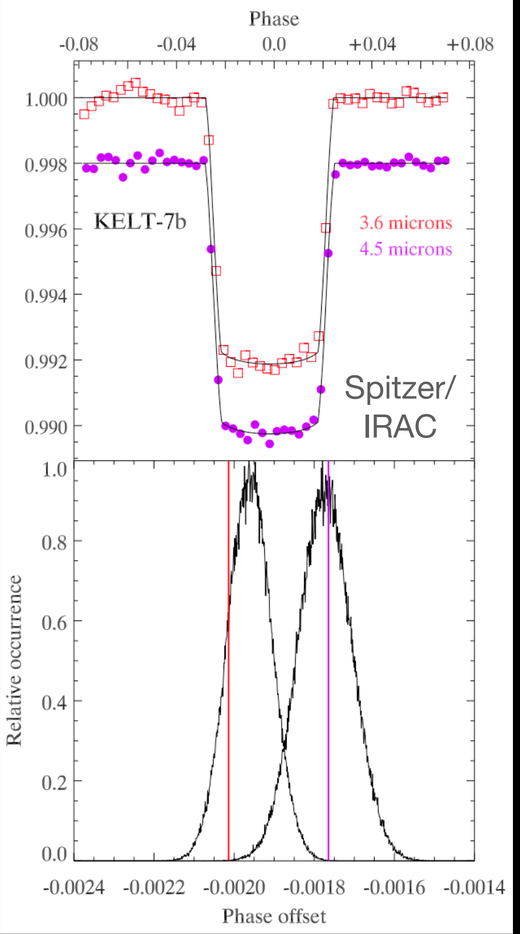

Atmosphere modeling

The fitted (CHEOPS + TESS) and collected (HST + Spitzer) transit/occultation depths were analyzed further.

The overall strategy:

1.) emission spectroscopy: only HST and Spitzer infrared data,
transmission spectroscopy: all data,
2.) Bayesian retrievals (Pyrat Bay, Platon),
3.) equivalent model assumptions,
4.) system parameters from Bieryla et al. 2015,
5.) free + equilibrium-chemistry parameterization.

Equilibrium chemistry (ECH):

- the atmosphere is in termochemical equilibrium (no vertical mixing, photochemistry, ionization, or condensation),
- the molecular mixing ratios X_{g} are computed uniquely from tables (e.g., GGchem, FastChem),
- retrieves the metallicity [M/H] and C/O ratio.

Free chemistry (FCH):

- this approach does not assume equilibrium (there is vertical mixing, photochemistry, ionization, or condensation),
- the molecular mixing ratios X_{g} are computed as free parameters,
- retrieves the abundance of each molecule independently.

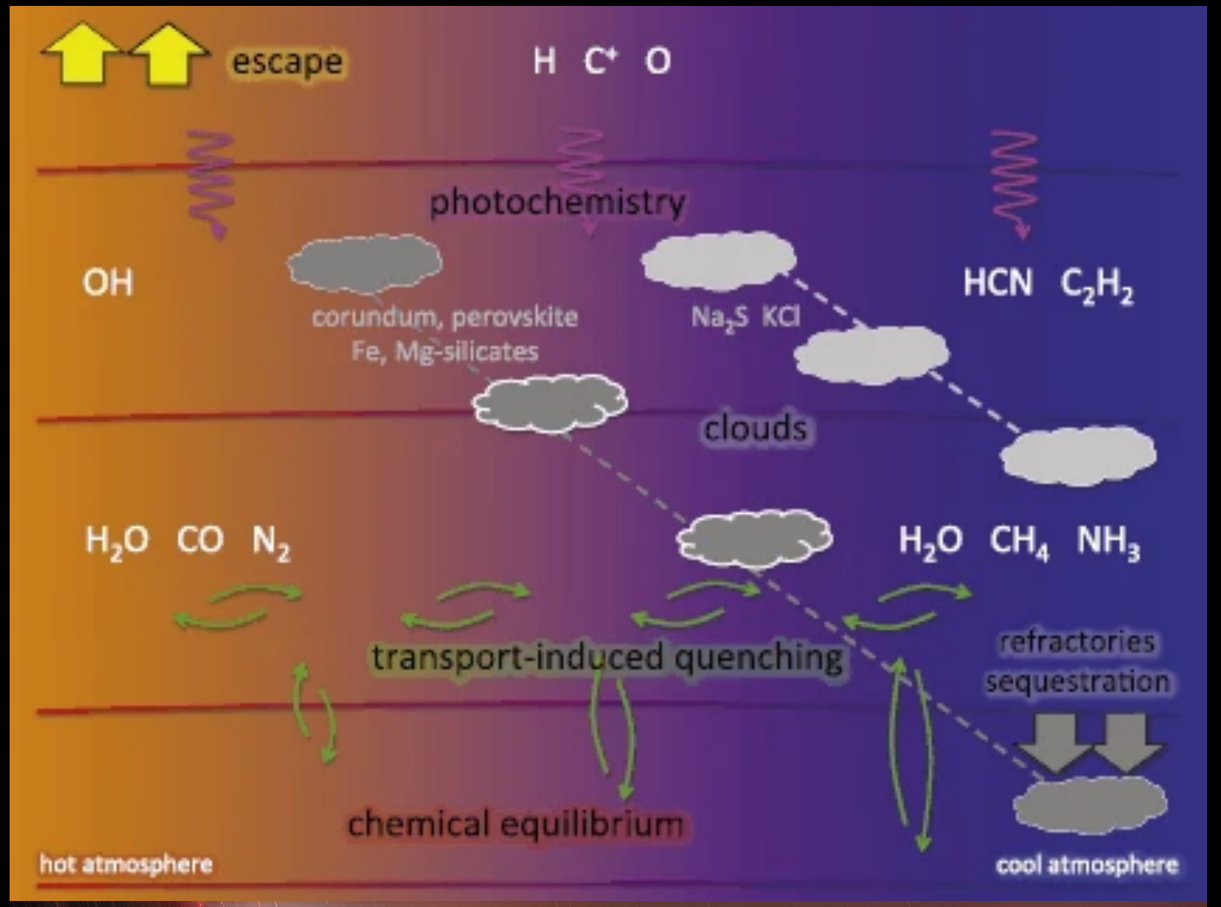

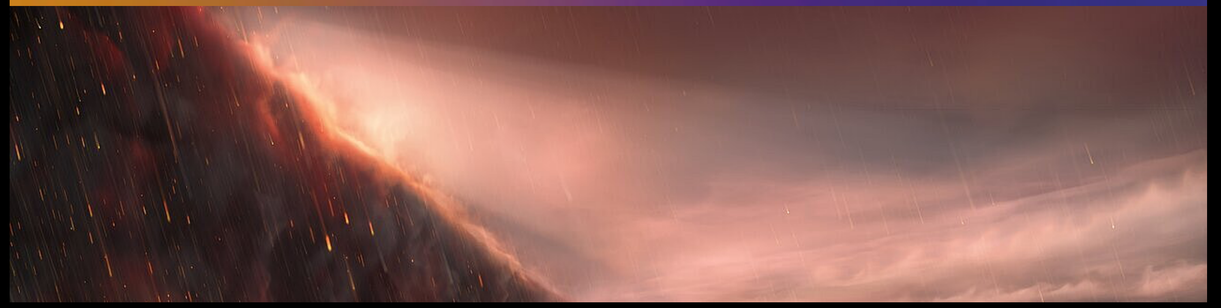

Table 5. Priors and posterior parameter estimations (median and 68% credible intervals) for the atmospheric retrievals.

	PYRAT BAY retrievals			PLATON retrievals		
Parameter	Prior	Equilibrium	Free-chemistry	Prior	Equilibrium	Free-chemistry
Occultation						
$\log p_1$	$\mathcal{U}(-9, 2)$	$-2.2^{+1.9}_{-3.9}$	$-6.2^{+1.4}_{-1.3}$	$\mathcal{U}(-9, 1)$	$5.4^{+1.7}_{-6.3}$	$-1.5^{+1.9}_{-1.4}$
$\log p_2$	$\mathcal{U}(-9, 2)$	$-5.9^{+2.9}_{-2.0}$	$-0.2^{+1.4}_{-2.5}$	...	...	...
$\log p_3$	$\mathcal{U}(-9, 2)$	$0.65^{+0.89}_{-1.14}$	$-0.5^{+1.7}_{-1.9}$	$\mathcal{U}(-9, 1)$	$3.5^{+2.8}_{-4.7}$	$5.0^{+1.7}_{-1.8}$
a_1	$\mathcal{U}(0.2, 2.0)$	$1.27^{+0.48}_{-0.31}$	$1.33^{+0.41}_{-0.48}$	$\mathcal{U}(0.2, 2)$	$0.871^{+0.292}_{-0.091}$	$1.19^{+0.47}_{-0.41}$
a_2	$\mathcal{U}(0.2, 2.0)$	$0.78^{+0.41}_{-0.27}$	$0.69^{+0.18}_{-0.17}$	$\mathcal{U}(0.2, 2)$	$1.16^{+0.54}_{-0.56}$	$1.32^{+0.39}_{-0.42}$
T_0 (K)	$\mathcal{U}(500, 5000)$	2284^{+50}_{-73}	2650^{+130}_{-150}	$\mathcal{U}(X, X)$	2059^{+97}_{-102}	2695^{+157}_{-185}
T_3 (K)	...	...	...	$\mathcal{U}(500, 3000)$	2232^{+543}_{-1114}	2218^{+76}_{-110}
[M/H]	$\mathcal{U}(-1, 3)$	$2.60^{+0.29}_{-0.51}$	...	$\mathcal{U}(-2, 3)$	$2.22^{+0.46}_{-0.48}$	...
C/O	$\mathcal{U}(0.01, 2.0)$	$1.66^{+0.23}_{-0.31}$	...	$\mathcal{U}(0.001, 2)$	$1.64^{+0.23}_{-0.30}$	...
$\log X_{\rm H2O}$	$\mathcal{U}(-12, -1)$	...	$-6.9^{+3.3}_{-3.0}$	$\mathcal{U}(-12, -2)$	...	$-7.5^{+2.6}_{-2.7}$
$\log X_{\rm CO}$	$\mathcal{U}(-12, -1)$	...	$-6.8^{+3.2}_{-3.1}$	$\mathcal{U}(-12, -2)$	...	$-7.5^{+2.8}_{-2.7}$
$\log X_{\rm CO2}$	$\mathcal{U}(-12, -1)$	...	$-7.6^{+3.6}_{-2.6}$	$\mathcal{U}(-12, -2)$	...	$-8.5^{+2.1}_{-2.0}$
$\log X_{\rm CH4}$	$\mathcal{U}(-12, -1)$	...	$-4.4^{+2.3}_{-4.8}$	$\mathcal{U}(-12, -2)$	...	$-7.2^{+2.4}_{-2.9}$
$\log X_{\rm TiO}$	$\mathcal{U}(-12, -1)$	...	$-2.4^{+0.8}_{-5.8}$	$\mathcal{U}(-12, -2)$	...	$-3.3^{+0.8}_{-1.0}$
$\log X_{\rm VO}$	$\mathcal{U}(-12, -1)$	...	$-3.5^{+1.1}_{-5.7}$	$\mathcal{U}(-12, -2)$	...	$-5.0^{+0.9}_{-1.1}$
$\log X_{\rm FeH}$	$\mathcal{U}(-12, -1)$	...	$-7.6^{+3.9}_{-2.8}$	$\mathcal{U}(-12, -2)$	...	$-7.2^{+3.1}_{-2.8}$
$\log X_{\rm e-}$	$\mathcal{U}(-12, -1)$	...	$-6.8^{+3.5}_{-3.2}$	$\mathcal{U}(-12, -2)$	...	$-7.2^{+3.0}_{-2.9}$
$\log X_{\rm H}$	$\mathcal{U}(-12, -1)$	...	$-6.8^{+3.4}_{-3.1}$	$\mathcal{U}(-12, -2)$	...	$-7.1^{+2.9}_{-2.9}$
Transmission						
$T_{\rm iso}$ [K]	$\mathcal{U}(200, 3500)$	721^{+263}_{-402}	2094^{+248}_{-340}	$\mathcal{U}(200, 3000)$	496^{+416}_{-157}	981^{+179}_{-162}
$R_{\rm p}$ ($R_{\rm Jup}$)	$\mathcal{U}(0.65, 1.94)$	$1.4861^{+0.0042}_{-0.0091}$	$1.431^{+0.012}_{-0.011}$	$\mathcal{U}(0.65, 1.94)$	$1.486^{+0.004}_{-0.006}$	$1.486^{+0.007}_{-0.008}$
[M/H]	$\mathcal{U}(-1, 3)$	$1.47^{+0.66}_{-0.79}$	...	$\mathcal{U}(-2, 3)$	$1.36^{+0.64}_{-0.87}$	...
C/O	$\mathcal{U}(0.01, 2.0)$	$0.30^{+1.18}_{-0.25}$	...	$\mathcal{U}(0.001, 2)$	$0.48^{+1.06}_{-0.43}$	...
$\log X_{\rm H2O}$	$\mathcal{U}(-12, -1)$	...	$-3.18^{+0.50}_{-0.51}$	$\mathcal{U}(-12, -2)$	...	$-2.4^{+0.3}_{-0.5}$
$\log X_{\rm CO}$	$\mathcal{U}(-12, -1)$	...	$-6.8^{+2.9}_{-3.1}$	$\mathcal{U}(-12, -2)$	...	$-7.3^{+2.9}_{-3.0}$
$\log X_{\rm CO2}$	$\mathcal{U}(-12, -1)$	...	$-8.2^{+2.0}_{-2.3}$	$\mathcal{U}(-12, -2)$	...	$-7.8^{+2.4}_{-2.5}$
$\log X_{\rm CH4}$	$\mathcal{U}(-12, -1)$	...	$-8.5^{+2.1}_{-2.1}$	$\mathcal{U}(-12, -2)$	...	$-9.0^{+1.9}_{-1.9}$
$\log X_{\rm TiO}$	$\mathcal{U}(-12, -1)$	...	$-10.88^{+0.88}_{-0.71}$	$\mathcal{U}(-12, -2)$	...	$-10.9^{+0.8}_{-0.7}$
$\log X_{\rm VO}$	$\mathcal{U}(-12, -1)$	...	$-10.50^{+1.04}_{-0.94}$	$\mathcal{U}(-12, -2)$	...	$-10.8^{+0.9}_{-0.8}$
$\log X_{\rm FeH}$	$\mathcal{U}(-12, -1)$	...	$-2.6^{+0.5}_{-0.6}$	$\mathcal{U}(-12, -2)$	...	$-7.6^{+2.9}_{-2.8}$
$\log X_{\rm e-}$	$\mathcal{U}(-12, -1)$	...	$-6.9^{+3.2}_{-3.2}$	$\mathcal{U}(-12, -2)$	...	$-4.3^{+1.4}_{-2.3}$
$\log X_{\rm H}$	$\mathcal{U}(-12, -1)$	...	$-7.0^{+3.3}_{-3.0}$	$\mathcal{U}(-12, -2)$	...	$-4.3^{+1.5}_{-2.4}$
$\alpha_{\rm ray}$	$\mathcal{U}(-10, 0)$	$-5.7^{+3.7}_{-3.0}$	$-8.4^{+2.0}_{-1.1}$	$\mathcal{U}(-10, 0)$	$-4.5^{+3.0}_{-4.5}$	$496^{+2.9}_{-3.2}$
$\log \kappa_{\rm ray}$	$\mathcal{U}(-3, 5)$	$-0.8^{+1.8}_{-1.5}$	$2.56^{+0.66}_{-0.96}$	$\mathcal{U}(-3, 5)$	$-1.47^{+1.22}_{-1.00}$	$-1.1^{+1.3}_{-1.1}$
$\log p_{\rm cloud}$	$\mathcal{U}(-7, 2)$	$-0.6^{+1.7}_{-1.9}$	$-0.2^{+1.3}_{-1.4}$	$\mathcal{U}(-5.99, 0)$	$-0.64^{+0.46}_{-0.84}$	$-0.92^{+0.57}_{-0.73}$

Notes. Using PYRAT BAY and PLATON, assuming thermochemical-equilibrium and free-chemistry abundances. $X_{\rm s}$ denotes the volume mixing ratio for the given species. All pressure values are in bar units.

Equlibrium chemistry vs Free chemistry

Pluriel et al. (2020) and Changeat et al. (2022):
- with FCH, they found an inverted T-P profile,
- non-detection of H_2O,
- detection of H^- absorption.

Metallicity [M/H] — only in the equilibrium-chemistry case

C/O ratio — only in the equilibrium-chemistry case

Mixing ratio of species $X_{\rm g} = \frac{n_{\rm g}}{n_{\rm total}}$ (in log scale) — only in the free-chemistry case

Results:

Both retrieval codes produce consistent results.

Occultations:

- ECH: C/O > 1 and a super-solar metallicity [M/H], with a relatively weak H_2O absorption at $1.4\,\mu$m,
- FCH: strong optical absorbers, TiO and VO, are the only species with well-constrained abundances, albeit at — likely unphysically — high concentrations, H_2O abundance less than ~10-100 ppm.

Transits:

- ECH: C/O < 1 and super-solar metallicity [M/H],
- FCH: both retrievals detect H_2O, and an additional optical absorber — Pyrat Bay: FeH and hazes, Platon: H^- absorption.

Equlibrium chemistry vs Free chemistry

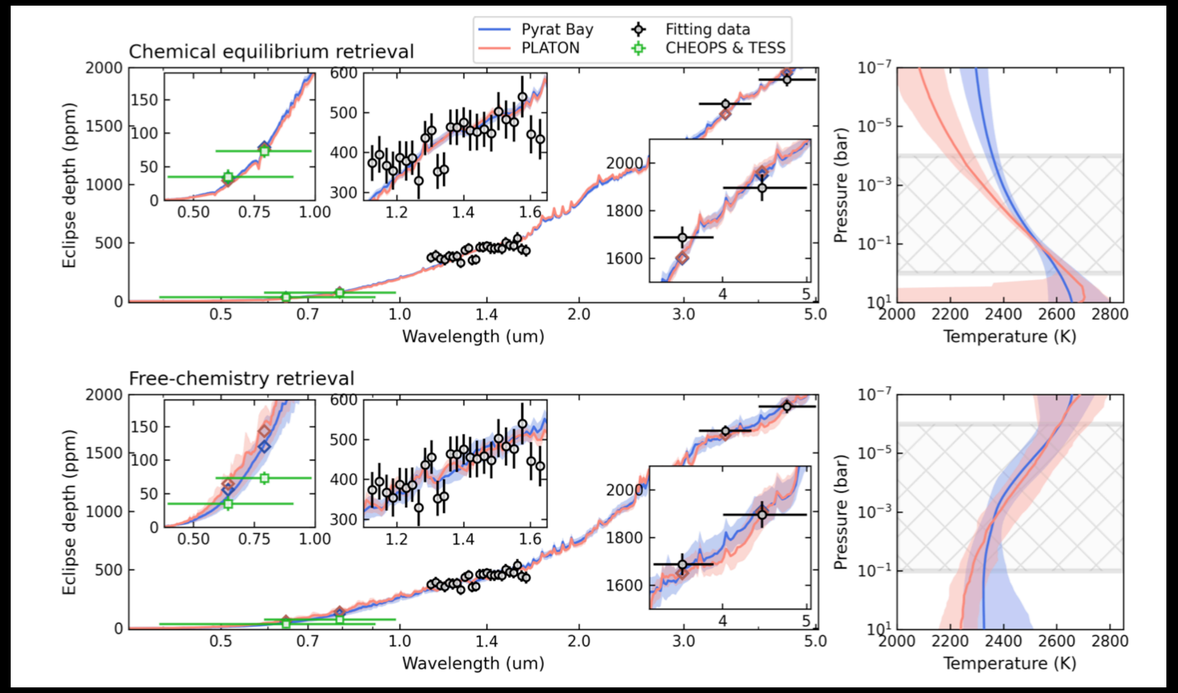

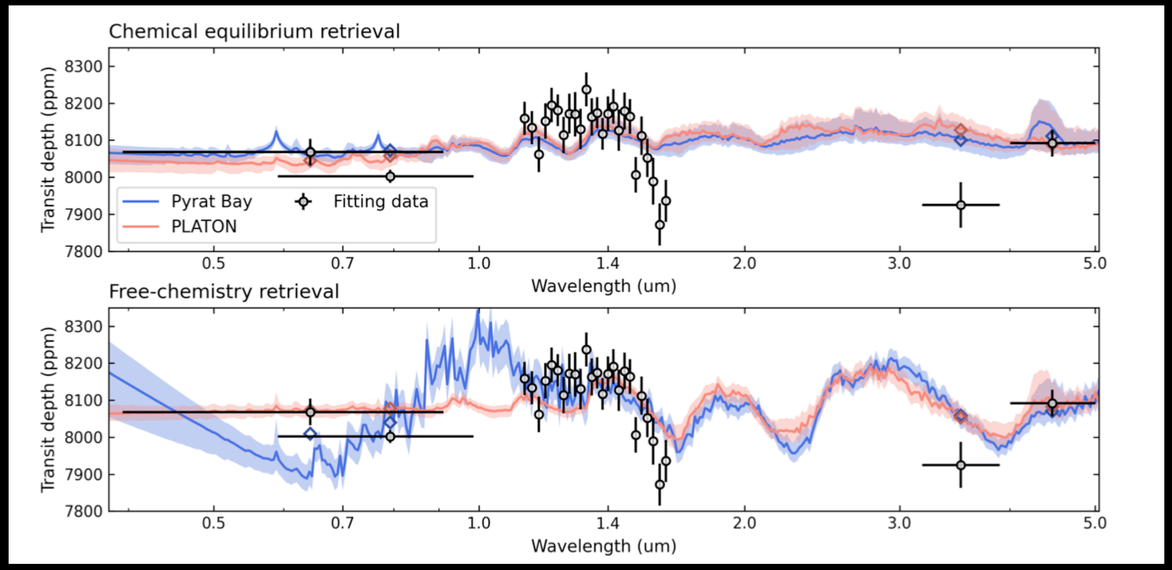

Emission retrievals

Transmission retrievals

- Thermochemical equilibrium: a non-inverted T-P profile,
- free-chemistry atmospheric parametrization: an inverted T-P profile,
- our FCH results are well in agreement with the previously published FCH results, except for the optical absorber,
- FCH retrievals generally yield better fits to the observations than ECH.

Configuration tests:

1.) different system parameters,
2.) different thermal parametrization,
3.) smaller vs larger set of absorbers,
but no qualitative differences:
FCH vs ECH is the main factor determining the results.

We adopted ECH retrieval results as our final results, because:

1.) assuming FCH risks adopting unphysical scenarios,
2.) disECH processes become less important at high *T*,
3.) if disECH occurs at all, it would occur in high altitudes, above the pressures probed by the observations.

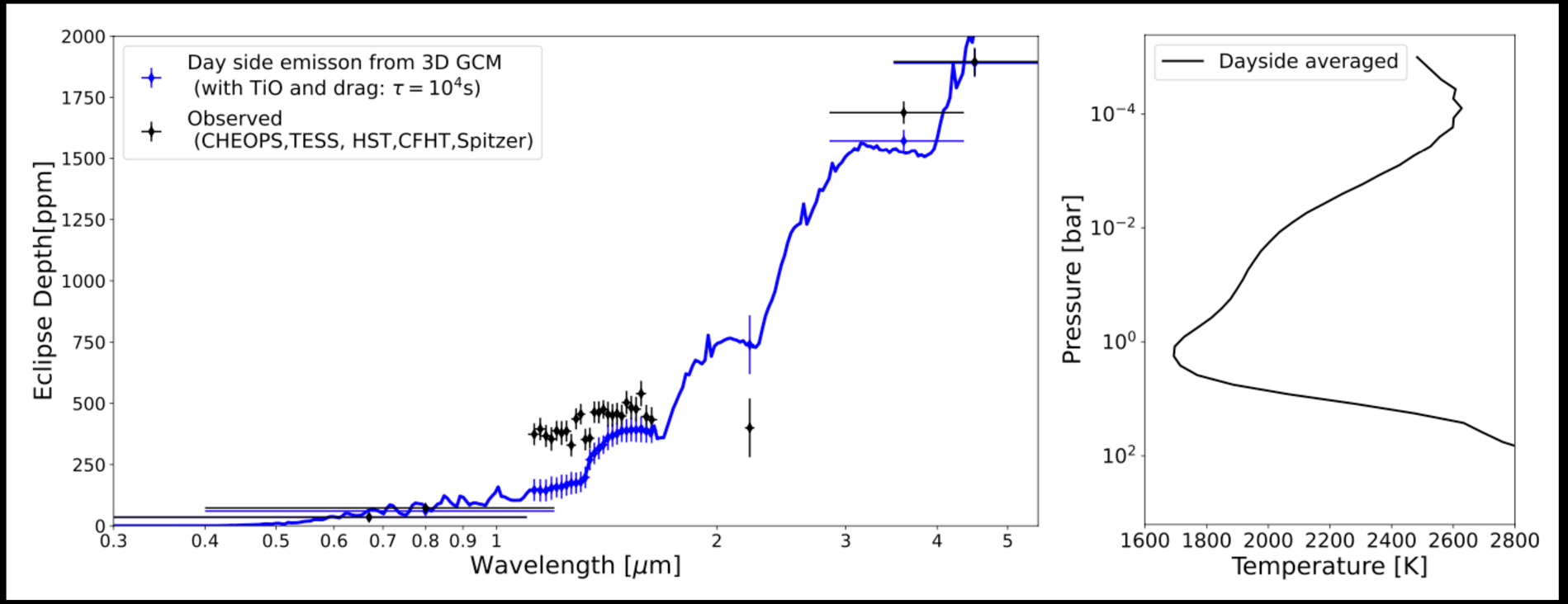

3D atmosphere modeling with a general circulation model (GCM)

- We also simulated the dayside of the planet with a 3D GCM expeRT/MITgcm/ExoRad (Carone et al. 2020):
- to match the eclipse depths in the CHEOPS, TESS, HST, and Spitzer passbands, TiO and VO opacities, and strong magnetic drag are needed.

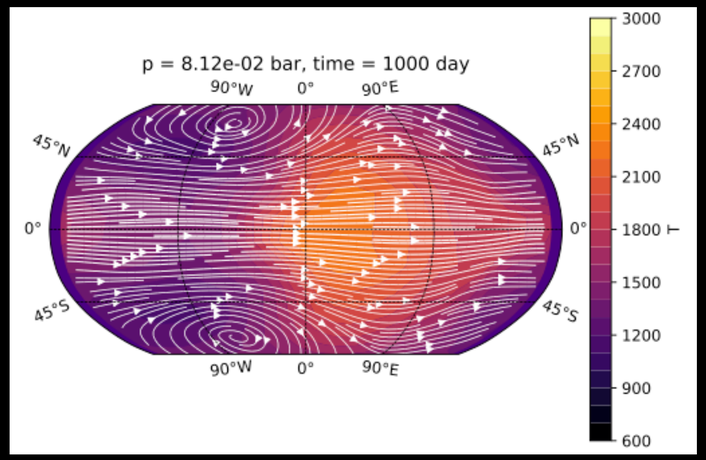

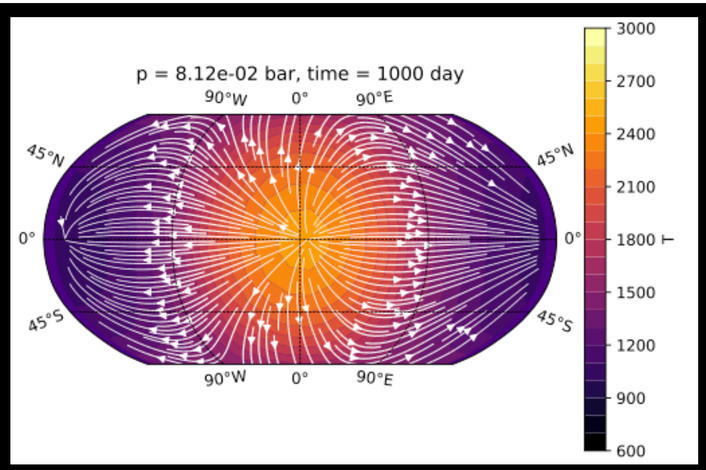

<u>Given the limited data, we only tested:</u>

1.) a model without TiO and without drag,
2.) a model with TiO and without drag,
3.) a model with TiO and with drag;
we used the smallest drag that effectively disrupts superrotation.

- Although we selected the best model, it significantly underestimates the HST data,
- the 3D GCM yields a T-P inverted profile that was not recovered with the retrieval models in ECH, only in the case of FCH,
- these models, however, use mainly the HST data, which disagree with the predictions of the 3D GCM model,
- the 3D GCM model yields inefficient horizontal heat redistribution ϵ, which is consistent with the albedo results.

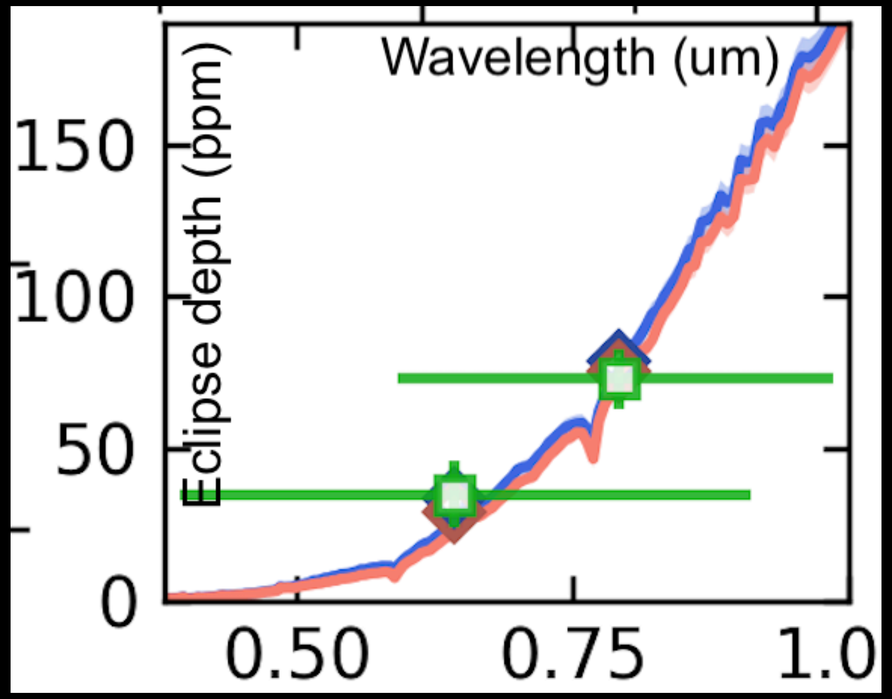

Extending the ECH retrieval emission models over the CHEOPS and TESS optical passbands:

- the thermal emission from the planet is consistent with the observed occultation depths in these passbands → the planet has a low geometric albedo producing little reflected light.

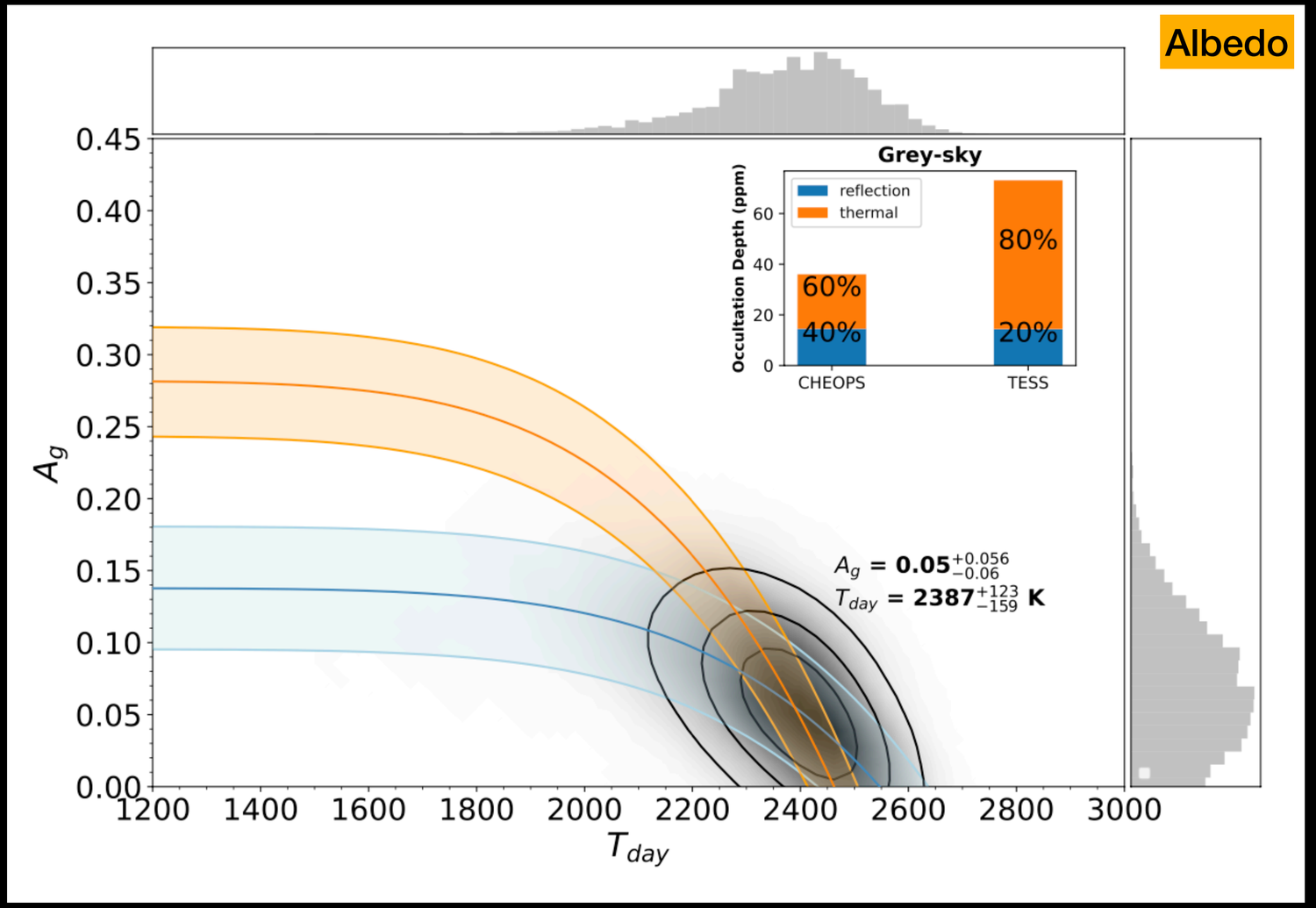

- The occultation depth can be expressed as the sum of the thermal emission and reflection: $D_{\rm occ} = E(T_{\rm day}) + R(A_{\rm g})$,

- we disentangled $E(T_{\rm day})$ and $R(A_{\rm g})$ by assuming a gray-sky atmosphere,

such that $T_{\rm day}$ and $A_{\rm g}$ are identical in the CHEOPS and TESS passbands (Singh et al. 2024),

- we obtained a very low geometric albedo of $A_{\rm g} = 0.05 \pm 0.06$, which corresponds to

a brightness temperature of $T_{\rm day} = 2387^{+123}_{-159}$ K, consistent with $\epsilon \approx 0$, with the ECH retrievals, and the 3D GCM.

Discussion points

- The FCH retrievals provide better fits to the observations, than the ECH retrievals,
- the large $T_{\rm day}$ variation of ~400 K in a narrow λ range suggests, however, an additional problem with the HST data,
- given the host is a spotted rapidly-rotating F2V-type star, the appearance and disappearance of star spots lead to nontrivial changes in the HST/WFC3 data during the observation.

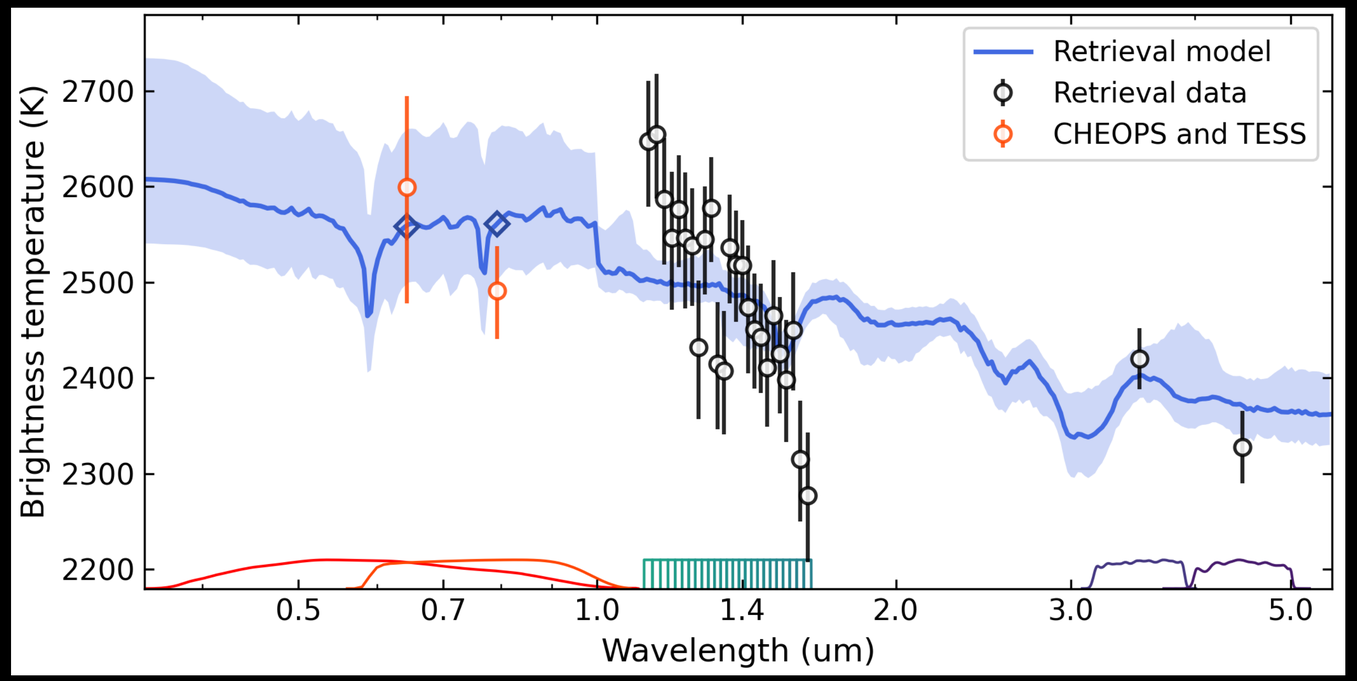

The Pyrat Bay ECH emission retrieval model converted from $D_{\rm occ}(\lambda)$ to $T_{\rm day}(\lambda)$.

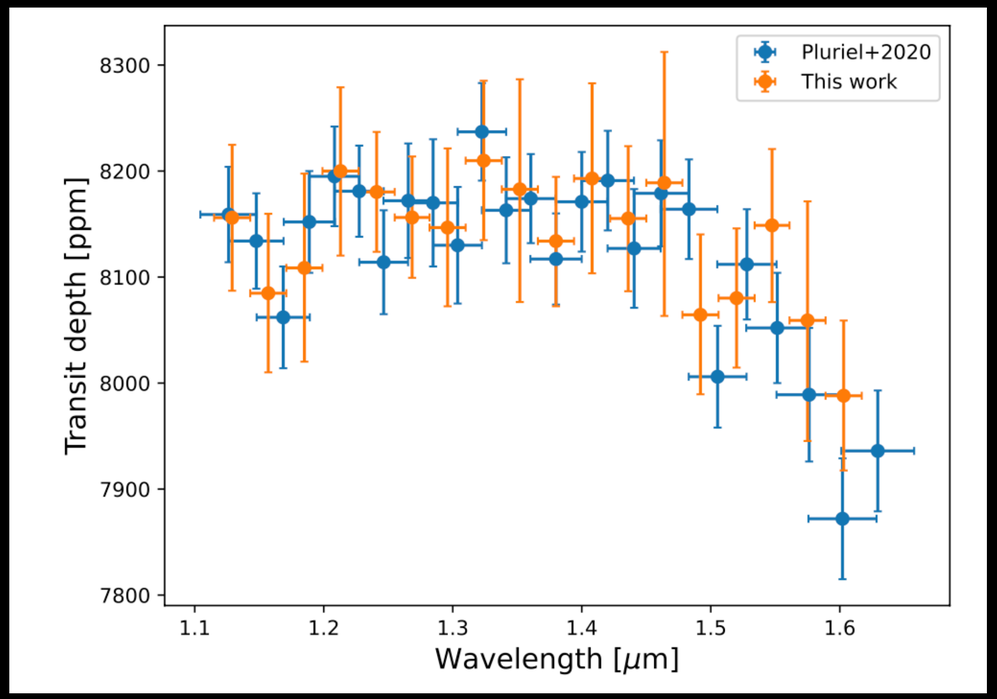

- To test this scenario, we independently reduced the HST/WFC3 transit data and compared the output to the data presented previously by Pluriel et al. (2020),
- no significant differences → we cannot explain the poor fit with instrumental artifacts.

- We applied **coherent stellar variability treatment** on TESS and CHEOPS data; HST/WFC3 data would also benefit from a similar treatment as proposed by Saba et al. (2025).

Summary and Conclusions

- **Occultation depths of KELT-7b:** $D_{\mathrm{occ,CHEOPS}} = 36 \pm 11\,\mathrm{ppm}$, $D_{\mathrm{occ,TESS}} = 69 \pm 9\,\mathrm{ppm}$.
- **Conclusion:** KELT-7b has shallow eclipses → characteristic of hot Jupiters in optical passbands (typically < 100 ppm).

- **Thermochemical-equilibrium atmospheric composition → a non-inverted T-P profile** (in contrast with previous results).
- **Free-chemistry atmospheric parameterization → an inverted T-P profile** (unphysically high TiO + VO concentrations).
- **Conclusion:** Configuration tests → the choice of FCH or ECH is the main factor determining the results.
- Free-chemistry retrievals generally yield better fits; however, assuming free chemistry risks adopting unphysical scenarios for ultrahot Jupiters, such as KELT-7b.

- **The 3D GCM results support a TiO-induced temperature inversion** (in tension with the ECH retrieval results).
- **Conclusion:** The retrievals focus on the HST data, while the 3D GCM focuses on the CHEOPS, TESS, and Spitzer data.

- **Every model fits the HST data poorly** + high brightness temperature gradient + no difference in HST data reduction.
- **Conclusion:** There might be a problem with the HST/WFC3 data in the case of this particular planet (stellar activity).
- HST/WFC3 observations would also benefit from a coherent treatment of stellar variability.

- **We report for KELT-7b a very low geometric albedo** $A_{\mathrm{g}} = 0.05 \pm 0.06$ in the CHEOPS + TESS passband.
- **Conclusion:** This result supports previous observations that hot Jupiters generally have low geometric albedos.
- The very low geometric albedo is consistent with inefficient heat redistribution, with the ECH retrievals, and the 3D GCM.
- The planet effectively absorbs nearly all incoming stellar irradiation to heat its dayside atmosphere.


Thank you!